

Optimization of electric and magnetic field intensities in proximity of power lines using genetic and particle swarm algorithms

KRZYSZTOF KRÓL, WOJCIECH MACHCZYŃSKI

*Institute of Electrical Engineering and Electronics, Poznan University of Technology
Piotrowo 3A, 60-965 Poznań, Poland
e-mail: krzykrol6@wp.pl, Wojciech.Machczynski@put.poznan.pl*

(Received: 18.06.2018, revised: 21.08.2018)

Abstract: The paper presents optimization of power line geometrical parameters aimed to reduce the intensity of the electric field and magnetic field intensity under an overhead power line with the use of a genetic algorithm (AG) and particle swarm optimization (PSO). The variation of charge distribution along the conductors as well as the sag of the overhead line and induced currents in earth wires were taken into account. The conductor sag was approximated by a chain curve. The charge simulation method (CSM) and the method of images were used in the simulations of an electric field, while a magnetic field were calculated using the Biot–Savart law. Sample calculations in a three-dimensional system were made for a 220 kV single – circuit power line. A comparison of the used optimization algorithms was made.

Key words: power line, electric field, magnetic field, optimization, genetic algorithm, particle swarm algorithm

1. Introduction

The increase of electric power demand has increased the need for transmitting huge amount of power over long distances. Transmission lines with high voltage and current levels generate large values of electric and magnetic fields intensities of which can affect a human being [9, 15–17, 25, 27, 29] and nearby objects. It is usually required to reduce the intensity of fields produced by power lines. Therefore studies of calculation techniques to accurately predict the optimal distribution of electric and magnetic field intensities are considered as necessary and important objects of efforts to manage electric and magnetic fields in the vicinity of high voltage power lines.

The electric field intensity is a function of the line voltage, but its resolution depends on terrain conditions, wires deployment, wire suspension height, conductor lengths, phase order and

phase voltage, and the intensity of the magnetic field depends on the currents flowing in the phase conductors, currents induced in the earth wires. The routes of power lines are designed in such a way that they bypass the urbanized areas, but often the lines pass near or over residential buildings. In the Regulation of the Minister of the Environment [18], the maximum permissible intensity for an electric field is defined as 10 kV/m for areas accessible to people, and for a place of residence 1 kV/m, while the value of magnetic field strength can not exceed 60 A/m. Power lines of the highest voltages in the case of approaching buildings meet the requirements for the magnetic field, the problem arises in the case of an electric field. In order to reduce the field strengths, it should be replaced by an overhead line with an underground cable, unfortunately this solution is expensive and not always possible. In [2, 5, 6] one can encounter field optimizations using the genetic algorithm (AG) [2, 6] or swarm particles (PSO) [5, 11] in a way that does not take into account significant factors as line sag, currents induced in earth wires, etc.

The aim of the paper is to present a model for calculating electric and magnetic field intensities, as accurate as it is possible, taking into account conductor sag, distribution of electric charges along line wires and currents in earth conductors, and then to present a calculation example, using GA and PSO algorithms. The example concerns the optimization (minimization) of electric field and magnetic field intensities in a specific area below the power line. The results using GA and PSO algorithms were compared.

2. Intensity of the electric and magnetic fields of a power line including the sag of wires

2.1. Calculation model of a sagging conductor

Simplified electric and magnetic field computation techniques assume that the power line conductors are straight wires of infinite length, parallel to each other, and located above and parallel to a flat ground plane. This assumption results in a model, the electric and magnetic fields of which are distorted from those produced in reality. In fact the conductors are periodic catenaries, the sag of which depends on individual characteristics of the line and on environmental conditions. The effect of the catenary on magnitudes of the electric and magnetic field intensities can be significant in some cases [14–16, 23–25, 30] and it has to be taken into account in the presented approach.

In a power transmission line the sag, depends on weather and terrain conditions. The height at the place of the largest sag depends on the type of line and is included in the standard PN-EN 50341. To take the sag into account in the calculations, divide a conductor of a span into n equal segments ($s_1, s_2, \dots, s_{i-1}, s_i, s_{i+1}, s_n$) as shown in Fig. 1. H is the maximum height of the conductors suspension, h is the minimum height of the conductors suspension in the middle of the span, S is the conductor sag, $S = H - h$. The calculations are based on the assumption that the number of simulation charges must correspond to the number of defined segments.

Each of the segments (s_1, \dots, s_n) can be described by the catenary equation [1, 2, 14, 22]:

$$z'(x') = h + 2\alpha \sinh^2\left(\frac{x'}{2\alpha}\right), \quad (1)$$

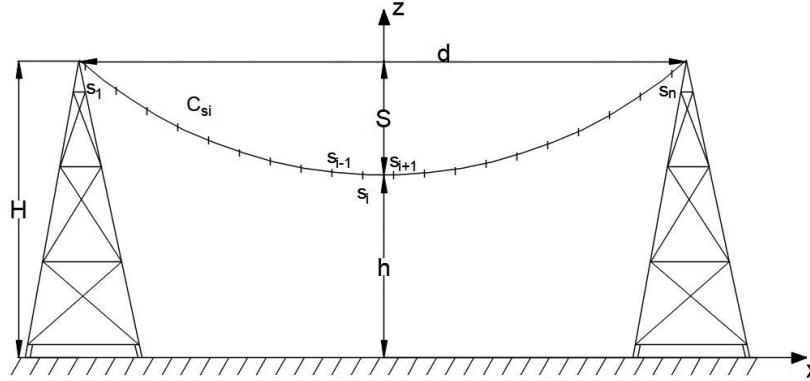


Fig. 1. Division of power line conductor with sag into n segments

where α is related to the mechanical parameters of the line: $\alpha = T_h/w$. T_h is the mechanical stress in the middle of the line, w is the weight per unit of the length of the line. This coefficient can be calculated recursively from the equation:

$$H = h + 2\alpha \sinh^2 \left(\frac{d}{2\alpha} \right). \quad (2)$$

2.2. Calculation of electric field intensity

The inputs to the calculation are data regarding voltage, circuit phasing, conductor sizes and locations. The potential of the static electric field near a power line at any observation point above the ground plane is determined by using the charge simulation method (CSM) [20] and the image method from Equation (3):

$$V_{si}(r) = \int_{C_{si}(r')} \frac{\lambda_{si}}{4\pi\epsilon_0} \frac{dl'_{si}}{R_{si}} - \int_{C_{si1}(r')} \frac{\lambda_{si}}{4\pi\epsilon_0} \frac{dl'_{si1}}{R_{si1}}, \quad (3)$$

where $\epsilon_0 = 8.854 \cdot 10^{-12}$ F/m is the electric permeability of the vacuum, λ is the line charge density (C/m) along the segment s_i . The first integral in (3) is calculated along the curve $C_{si}(r')$, $|R_{si}| = |r - r'|$, r' is the position of any point N on the curve $C_{si}(r')$ (source point), r is the position of the observation point P . The second integral in (3) – scalar potential created by the electric charges induced on the surface of the image curve $C_{si1}(r')$, $|R_{si1}| = |r - r'_1|$, r'_1 is the position of any point N' on the curve $C_{si1}(r'_1)$ (image point). The vectors of distances between the source point N and its image N' to the observation point P can be written as:

$$\mathbf{R}_{si} = (x - x')\mathbf{a}_x + (y - y')\mathbf{a}_y + (z - z')\mathbf{a}_z \quad (4)$$

and

$$\mathbf{R}_{si1} = (x - x')\mathbf{a}_x + (y - y')\mathbf{a}_y + (z - z')\mathbf{a}_z, \quad (5)$$

where (x, y, z) are the coordinates of the observation point P , and (x', y', z') are the coordinates of the source points, as shown in Fig. 2, \mathbf{a}_x , \mathbf{a}_y , \mathbf{a}_z are the unit vectors of the Cartesian coordinate system.

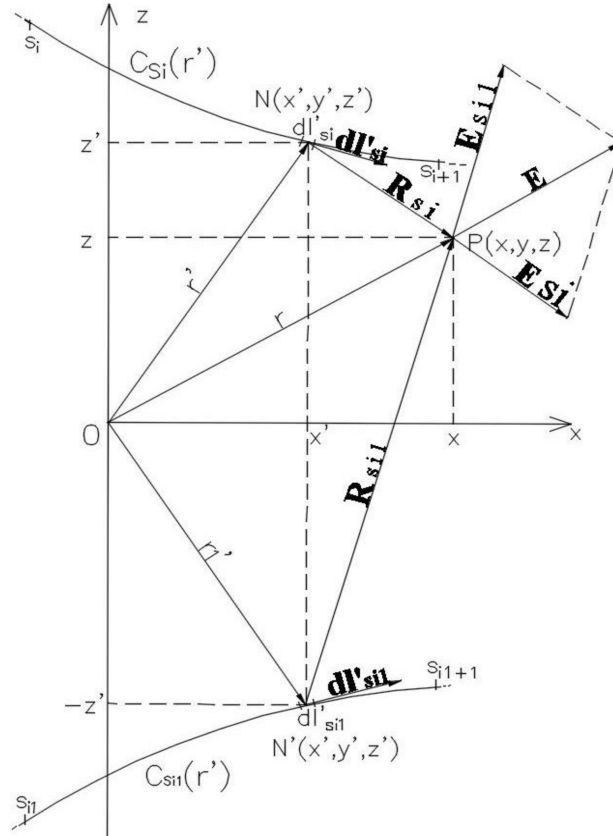


Fig. 2. Geometry of the system considered

The linear density of the charge of an individual segment is determined from matrix Equation (6):

$$\begin{bmatrix} \lambda_{s1} \\ \lambda_{s2} \\ \vdots \\ \lambda_{sn} \end{bmatrix} = 4\pi\epsilon_0 \begin{bmatrix} V_{s1} \\ V_{s2} \\ \vdots \\ V_{sn} \end{bmatrix} \begin{bmatrix} I1_{11} - I2_{11} & I1_{12} - I2_{12} & \dots & I1_{1n} - I2_{1n} \\ I1_{21} - I2_{21} & I1_{22} - I2_{22} & \dots & I1_{2n} - I2_{2n} \\ \vdots & \vdots & \ddots & \vdots \\ I1_{n1} - I2_{n1} & I1_{n2} - I2_{n2} & \dots & I1_{nn} - I2_{nn} \end{bmatrix}^{-1}, \quad (6)$$

where: V_s is the potential of the contour point located on the surface of segment s_i , $I1$ and $I2$ are integrals represented by Equations (7) and (8).

$$I1_{ij} = \int_{C_{si}} \frac{\cosh\left(\frac{x'_j}{\alpha}\right) dx'_j}{\sqrt{(x_i - x'_j)^2 + (y_i - y'_j)^2 + \left(z_i - h - 2\alpha \sinh^2\left(\frac{x'_j}{2\alpha}\right)\right)^2}}, \quad (7)$$

$$I_{2ij} = \int_{C_{si}} \frac{\cosh\left(\frac{x'_j}{\alpha}\right) dx'_j}{\sqrt{(x_i - x'_j)^2 + (y_i - y'_j)^2 + \left(z_i - h - 2\alpha \sinh^2\left(\frac{x'_j}{2\alpha}\right)\right)^2}}. \quad (8)$$

In the case where the power line consists of more than one conductor ($m = 1, 2, \dots, M$), the charges caused on the n segments of the conductor m are calculated from dependence (9):

$$\begin{bmatrix} [V_s]_{11} \\ [V_s]_{12} \\ \vdots \\ [V_s]_{M1} \end{bmatrix} = \frac{1}{4\pi\epsilon_0} \begin{bmatrix} [P_s]_{11} & [P_s]_{12} & \dots & [P_s]_{1n} \\ [P_s]_{21} & [P_s]_{22} & \dots & [P_s]_{2n} \\ \vdots & \vdots & \vdots & \vdots \\ [P_s]_{M1} & [P_s]_{M2} & \dots & [P_s]_{Mn} \end{bmatrix} \begin{bmatrix} [\lambda_s]_{11} \\ [\lambda_s]_{12} \\ \vdots \\ [\lambda_s]_{M1} \end{bmatrix}, \quad (9)$$

where $[P_s]_{ij}$ is the sub-matrix of the Maxwell's potential coefficients between the segments of the conductor i and those of the conductor j , $[\lambda_s]_{ij}$ is the sub-matrix of the induced charge along the segments of the conductor i , $[V_s]_{ij}$ is the voltage matrix between the wire segments i and the wire j .

Intensity of the electric field at any point above the earth's surface is represented by Equation (10):

$$\mathbf{E}(r') = \frac{\lambda_{si}}{4\pi\epsilon_0} \left(\int_{C_{si}(r')} \frac{\lambda_{si}(r')}{R_{si}^2} d\mathbf{l}'_{si} - \int_{C_{si}(r')} \frac{\lambda_{si}(r')}{R_{si}^2} d\mathbf{l}'_{si} \right). \quad (10)$$

The total electric field strength at the observation point is calculated from the vector summation of the fields from all the transmission line conductors, based on Formula (11):

$$\mathbf{E}_T(x, y, z) = c \sum_{m=1}^M \frac{1}{4\pi\epsilon_0} [\mathbf{I}_{3m} - \mathbf{I}_{4m}], \quad (11)$$

where

$$\mathbf{I}_{3m} = \int_{-d/2}^{d/2} \lambda_{sn}(r') \frac{\left((x - x')\mathbf{a}_x + (y - y')\mathbf{a}_y + (z - z')\mathbf{a}_z \right) \cosh\left(\frac{x'}{\alpha}\right)}{\left(\sqrt{(x - x')^2 + (y - y')^2 + (z - z')^2} \right)^3} dx', \quad (12)$$

$$\mathbf{I}_{4m} = \int_{-d/2}^{d/2} \lambda_{sn}(r') \frac{\left((x - x')\mathbf{a}_x + (y - y')\mathbf{a}_y + (z + z')\mathbf{a}_z \right) \cosh\left(\frac{x'}{\alpha}\right)}{\left(\sqrt{(x - x')^2 + (y - y')^2 + (z + z')^2} \right)^3} dx'. \quad (13)$$

2.3. Calculation of magnetic field intensity

The magnetic field of a power line is produced by currents flowing in phase conductors as well as in earth wires.

The method for calculating induced currents in earth wires, which uses the complex ground return plane approach was taken from [8, 14]. It should be noted that in the case, all conductors are considered as parallel to the earth surface, Fig. 3.

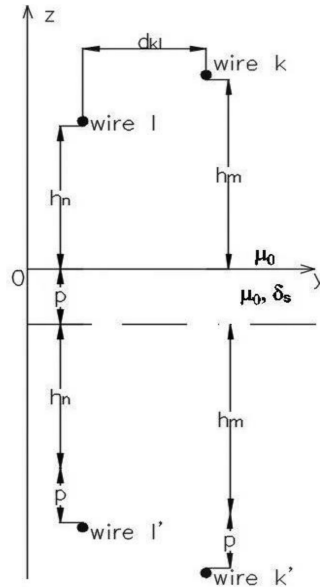


Fig. 3. Geometry of conductors k and l in the y, z plane

The current induced in earth wires, in the case of two earth wires k and l , can be calculated from the relation:

$$\begin{bmatrix} I_k \\ I_l \end{bmatrix} = - \begin{bmatrix} Z_k & Z_{kl} \\ Z_{kl} & Z_l \end{bmatrix}^{-1} \begin{bmatrix} Z_{1k} & Z_{2k} & Z_{3k} \\ Z_{1l} & Z_{2l} & Z_{3l} \end{bmatrix} \begin{bmatrix} I_1 \\ I_2 \\ I_3 \end{bmatrix}, \quad (14)$$

where I_k, I_l represent the currents (phasors) induced in earth wires k and l , I_1, I_2, I_3 are the phasors of the phase currents of the power line, $(Z_k, Z_l) - Z_s$ represent the complex self-impedance of the earth wire calculated from equations:

$$Z_s = j\omega \frac{\mu_0}{2\pi} \ln \frac{2(h+p)}{r}, \quad (15)$$

where h represents the height of an earth wire, r is the wire radius,

$$p = \frac{1}{\sqrt{j\omega\mu_0\gamma}} = \frac{\delta_s}{2}(1-j), \quad (16)$$

$$\delta_s = \frac{1}{\sqrt{\pi f \mu_0 \gamma}} \quad (17)$$

and γ is the ground conductivity, f is the frequency.

The mutual complex impedances (Z_m) between the power line conductors m and n can be obtained from the equation:

$$Z_m = j\omega \frac{\mu_0}{2\pi} \ln \frac{g}{a}, \quad (18)$$

$$g = \sqrt{(h_m + h_n + 2p)^2 + d_{mn}^2}, \quad (19)$$

$$a = \sqrt{(h_m - h_n)^2 + d_{mn}^2}, \quad (20)$$

where d_{mn} is the distance between the conductors m and n , h_m , h_n represent the height of the conductor m and n .

The magnetic flux density produced by the current in a single sagging conductor can be calculated using Biot–Savart’s law:

$$\mathbf{B}(r') = \mu_0 \left(\int_{C_{si}} \frac{I(l'_{si}) d\mathbf{l}'_{si} \times \mathbf{R}(l'_{si})}{4\pi |\mathbf{R}_{si}(l'_{si})|} \right), \quad (21)$$

where $\mu_0 = 4\pi \cdot 10^{-7}$ H/m is the magnetic permeability of the vacuum $I(l'_{si})$ current, $\mathbf{R}_{si}(l'_{si})$ is a vector from the source point to the observation point, $\mathbf{R}(l'_{si})$ is a unit vector in the direction of $\mathbf{R}_{si}(l'_{si})$. The intensity of the magnetic field at any point above the earth’s surface is determined from the relation:

$$\mathbf{H}(x, y, z) = \frac{1}{4\pi} \left[\int_{-d/2}^{d/2} \frac{((x-x')\mathbf{a}_x + (y-y')\mathbf{a}_y + (z-z')\mathbf{a}_z) \cosh\left(\frac{x'}{\alpha}\right)}{(\sqrt{(x-x')^2 + (y-y')^2 + (z-z')^2})^3} dx' \right]. \quad (22)$$

The total magnetic field is calculated from the vector summation of the fields from currents in all the transmission line conductors [1–3, 23, 26, 29]:

$$H_T = \sqrt{\sum_{m=1}^M H_x^2 + \sum_{m=1}^M H_y^2 + \sum_{m=1}^M H_z^2}. \quad (23)$$

3. Optimization of the electric and magnetic field intensity using a genetic algorithm (AG)

One of the methods used for optimization is a genetic algorithm, which find optimum solutions by mimicking the evolutionary processes of nature over a large number of generations [2, 6]. The height of the suspension of phase and earth wires, h is the minimum height of the suspension of the conductors in the middle of the span, the distance between the earth wires and the tower axis and the distance between the wires are parameters forming a population of chromosomes that initially consist of randomly selected real numbers in specific ranges. An initial population of possible solutions is developed randomly, where the genetic makeup of each individual in the population is an encoding of a possible solution to the problem. Subsequent generations are created by recombining the chromosomes of individuals in the parent population using the evolutionary operators of crossover, mutation, and selection. We can represent solutions of a given objective function as:

$$x = \{x_l, l = 1, 2, \dots, Nx\}. \quad (24)$$

The individual x_l (referred to as genes) contains the design variables, which are to be optimized and are usually encoded using a binary alphabet. Therefore, in the most common form, a gene can represent a discrete or discretized continuous value that can be real or complex. Genes are concatenated to form an individual's chromosome, denoted as:

$$p = \{g_l, l = 1, 2, \dots, Nl\}. \quad (25)$$

The genetic algorithm specifies the manner in which the genetic material of the initial population should be combined, removed, and mutated in order to stochastically find a globally optimal solution. Generally, after the fitness of each individual in the population has been calculated, the algorithm will select a certain number of individuals from the population based on their relative fitnesses. Typically, the better an individual's fitness is, the more likely it is to be chosen to pass on its genetic material to the next generation. The selected individuals ("parents") are then used to create the next generation by combining the chromosome of one individual with another, using the crossover operator. The algorithm iterates in this manner until the population has converged, hopefully on the globally optimal solution. The AG parameters to be considered for this optimal design problem are: population size $N = 40$, $x_l = 0.85$, $g_l = 0.07$. The flowchart of the AG operation presents Fig. 4 [7, 11, 13].

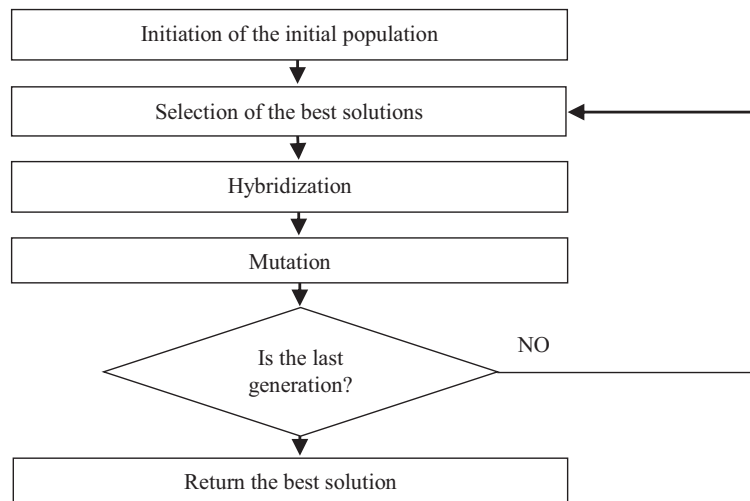


Fig. 4. Flowchart of the genetic algorithm (AG)

4. The swarm particle algorithm to optimize the electric and magnetic field intensities

Another algorithm that optimized the parameters of the power lines was the particle swarm optimization (PSO). This method is based on the observation of the social behavior of animals, such as a flock of birds and a school of fish. This method uses collaboration and sharing experience

with all population. A swarm consists of population who are called particles or agents. The PSO is a member of the class of nature-inspired meta-heuristic algorithms that has attracted a lot of attention in optimization research today [10, 12, 13]. The particles move to new locations, simulating the adaptation of the swarm to the environment. Each particle c is described by its position $X_c = (x_{c1}, x_{c2}, \dots, x_{cm})$, $c = 1, 2, \dots, N$ and speed $V_c = (v_{c1}, v_{c2}, \dots, v_{cm})$, $c = 1, 2, \dots, N$ and the solution of functions in m dimensional space is represented by a vector X_c . The swarm consists of n particles. Searching for the optimum function is carried out iteratively. In each iteration the swarm particle moves to a new position considering its old position and previous speed, as well as its best position found so far $P_c = (P_{c1}, P_{c2}, \dots, P_{cm})$, $c = 1, 2, \dots, N$ and the best position found in the entire swarm $G_c = (g_{c1}, g_{c2}, \dots, g_{cm})$, $g = 1, 2, \dots, N$. This own experience in the PSO is called a cognitive component. The speed of each particle can be calculated from the formula:

$$v_{(c,j)}^i = wv_cj^{(i-1)} + c_1r_1(P_{c,j} - x_{c,j}^{(i-1)}) + c_2r_2(G_{c,j} - x_{c,j}^{(i-1)}), \quad (26)$$

where $j = 1, \dots, m$, $I = 1, \dots, M$, M is the total number of individuals. c_1, c_2 are the learning rates, r_1, r_2 are the random numbers in the range $[0, 1]$. The inertia weight w modulates the influence of the former velocity and can be a constant or a decreasing function with values between 0 and 1. For example, [10, 13] used a linearly decreasing function over the specified time range with an initial value of 0.9 and an end value of 0.4. The position of the particle is determined by the formula:

$$x_{(c,j)}^i = x_{c,j}^{(i-1)} + v_{c,j}^i. \quad (27)$$

The flowchart of the PSO algorithm is shown in Fig. 5. A population size used in this paper is $N = 40$. In the initial implementation, the position of each searched variable was drawn and checked with the adopted assumptions, and w is equal to 1 [5, 10, 12, 13].

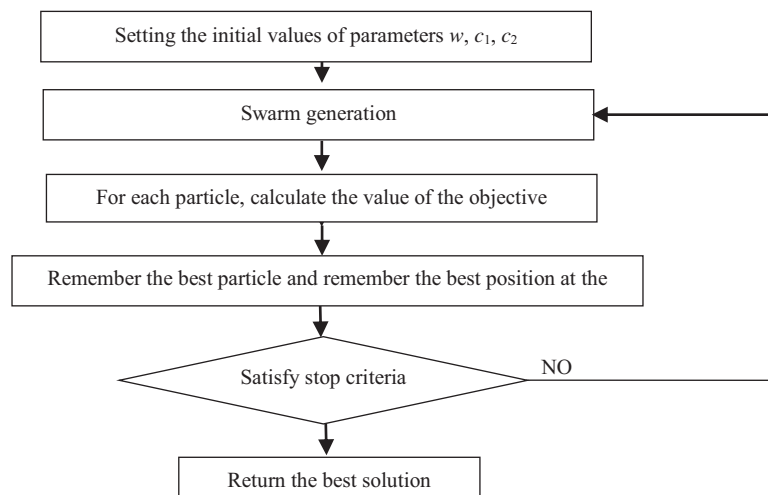


Fig. 5. Flowchart of the PSO algorithm

5. Optimization of magnetic and electric field intensities under a power line

The chosen power line had a rated voltage of 220 kV and was hung on the tower of type H52, characterized by the following parameters: the distance between the phase conductors $a = 7.6$ m, the height of the phase conductors $H_L = 26.5$ m, the height of the phase conductors in the center of the span $S_L = 6.7$ m, the height of the suspension of the earth wires $H_G = 30.6$ m, the height of the earth wires in the center tower of the span $S_G = 10.8$ m, the distance between the earth wires and the tower axis $o = 5.6$ m. The phase conductors are made are made of AFL-8 525 mm², and earth wires AFL-1.7 70 mm². Voltage configuration $\underline{U}_1 = 220e^{-j120^\circ}$ kV, $\underline{U}_2 = 220$ kV, $\underline{U}_3 = 220e^{j120^\circ}$ kV. The current of each phase conductor was 570 A. The length of the span of the line $d = 400$ m. The geometry of the line is shown in Fig. 6. The field intensity test was carried out at a height of 2 m, at a distance of ± 25 meters from the axis of the line at 20 000 points.

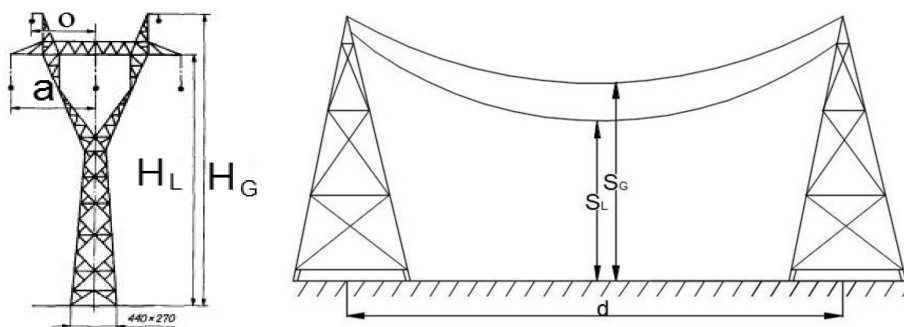


Fig. 6. Parameters of the 220 kV line

The maximum electric field strength (max RMS value) calculated according to Formula (11) is $E_{\max} = 5035.75$ V/m, while the maximum magnetic field strength (max RMS value) is $H_{\max} = 20.3$ A/m. The distribution of the electric field intensity is shown in Fig. 7, and the magnetic field intensity is shown in Fig. 8.

Objective function for the electric field intensity (max RMS value) is given by Equation (11) and for the magnetic field intensity (max RMS value) by Equation (23), respectively. Optimization was performed for the following assumptions:

- $E_{\max} < 1$ kV/m,
- $H_{\max} < 60$ A/m,
- $6 \text{ m} \leq a \leq 9 \text{ m}$,
- $18 \text{ m} \leq H_L \leq 26.5 \text{ m}$,
- $6 \text{ m} \leq S_L \leq 12 \text{ m}$,
- $4 \text{ m} \leq o \leq 7 \text{ m}$,
- $28 \text{ m} \leq H_G \leq 34 \text{ m}$,
- $10 \text{ m} \leq S_G \leq 12 \text{ m}$.

It should be noted, that the range of changes in the parameters to be optimized is consistent with the catalogue data of the power line under consideration.

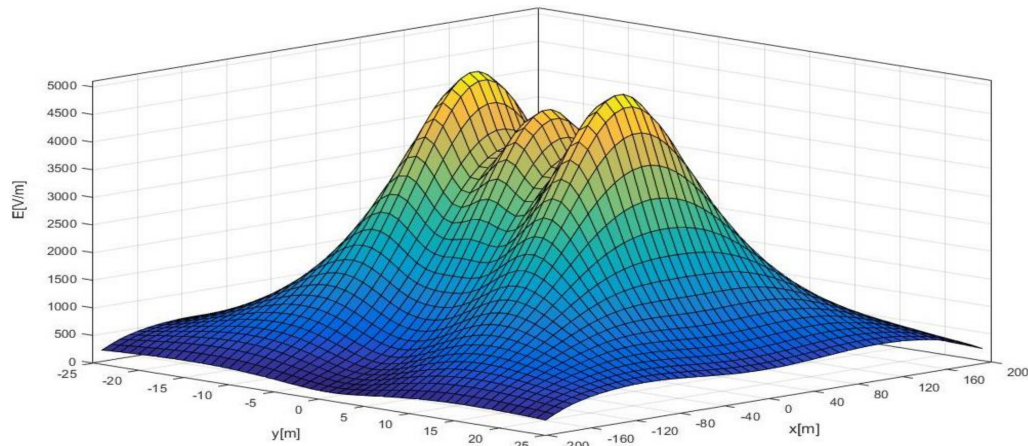


Fig. 7. Three-dimensional plot of the electric field intensity (max RMS value) under the 220 kV power line before optimization

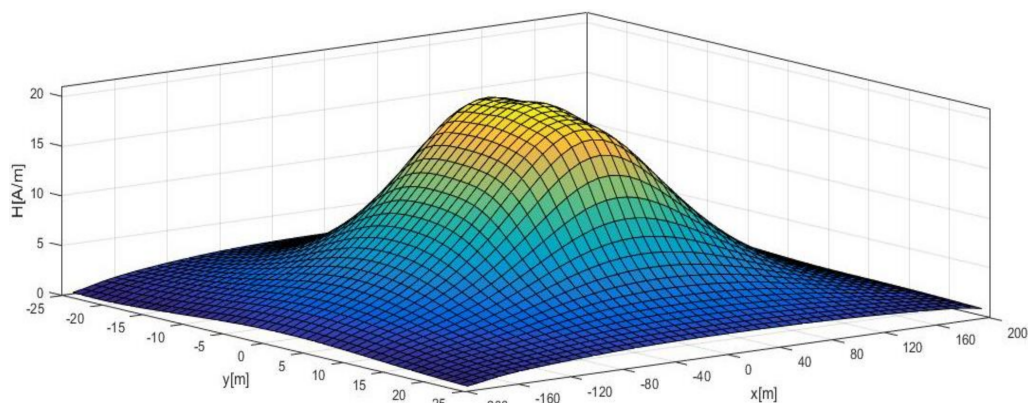


Fig. 8. Three-dimensional plot of magnetic field intensity (max RMS value) under the 220 kV power line before optimization

Table 1 presents the parameters of the line before and after the optimization. The maximum electric field (max RMS value) calculated by using the genetic algorithm is $E_{\max} = 696.698$ V/m, whereas $H_{\max} = 4.695$ A/m with earth wire currents I_e of $(15.69 + j23.68)$ A. The optimization was also made using the particle swarm algorithm. The maximum intensity (max RMS value) of the electric field was comparable to the value of the field intensity (max RMS value) obtained using the genetic algorithm and amounted to $E_{\max} = 688.592$ V/m, while $H_{\max} = 4.587$ A/m with earth wire currents of $(15.61 + j23.64)$ A. All results are summarized in Table 1.

The 3D plots of the intensity of the electric field intensity and the intensity of the magnetic field for both methods of optimization are similar and shown in Figs. 9 and 10, respectively.

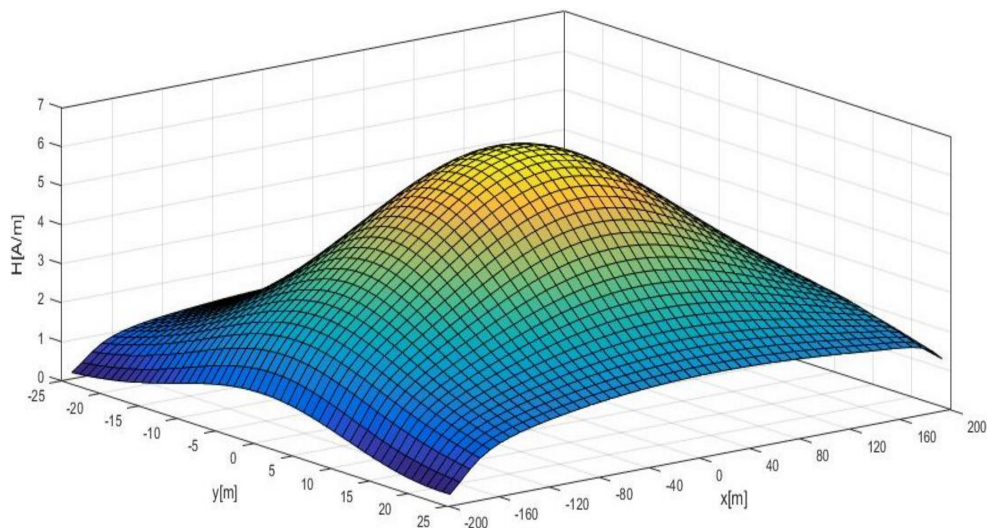


Fig. 9. Three-dimensional plot of the electric field intensity (max RMS value) under the 220 kV power line with optimized parameters

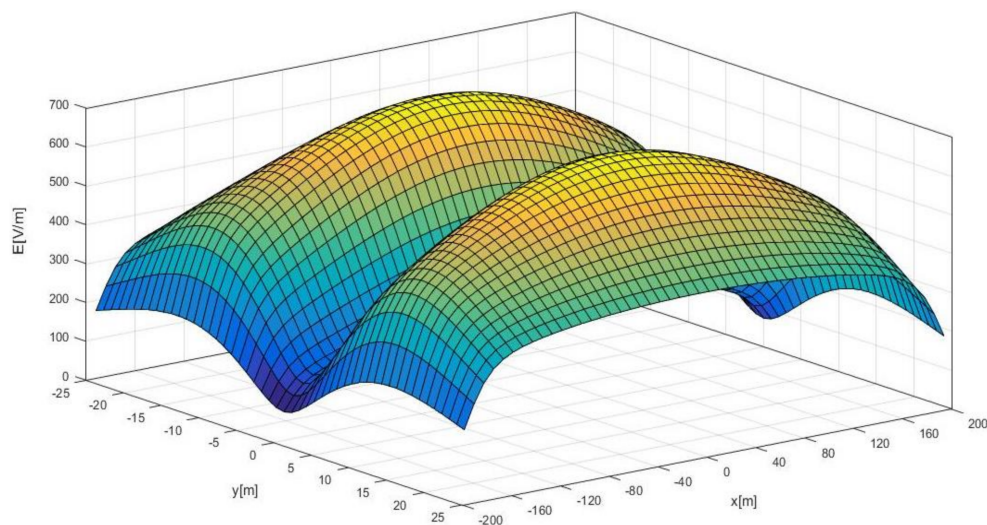


Fig. 10. Three-dimensional plot of the magnetic field intensity (max RMS value) under the 220 kV power line with optimized parameters

The time of calculating the electric field intensity using the genetic algorithm was 9560.88 seconds, while the PSO algorithm performed calculations in a shorter time of 3543.48 seconds. Calculations for 20 000 points were made on an Intel Core I7-6820HK machine with four cores of eight threads at 2.7 GHz and with 16 GB of RAM.

Table 1. Comparison of calculation results

	o [m]	a [m]	S_L [m]	H_L [m]	S_G [m]	H_G [m]	E_{\max} [V/m]	$I_{e1} \approx I_{e2}$ [A]	H_{\max} [A/m]
Before optimization	5.6	7.6	6.7	26.5	10.8	30.6	5035.75	$-14.36 - j117.24$	20.3
Genetic algorithm	4.320	6.210	14.012	24.124	19.125	27.879	696.698	$-15.69 + j23.68$	4.695
Particle swarm optimization	4.448	6.000	13.989	24.000	18.922	28.000	688.592	$-15.61 + j23.64$	4.587

6. Conclusions

The paper presents method of optimization the parameters of the power line using a genetic algorithm and a swarm of particles. In the case of the optimization of electric and magnetic fields beneath the power line the value of the electric field intensity after the optimization is three times smaller than with no optimization. Using the analyzed algorithms, similar optimization results were obtained, but the PSO algorithm allows one to obtain results three times faster than with the use of the AG, because the particles remember the information about the position gradient in the space sought. The speed of calculation also depends on the coupled systems of update equations because the particles exchange information.

According to the Regulation of the Minister of the Environment, the measurement of electric and magnetic field intensities must be carried out 2 m beneath the power line.

Future studies will have to apply the optimization method of electric and magnetic field intensity to a system with more than one power line and implement different voltages and conductor currents.

References

- [1] Dein A.Z., *Parameters affecting the charge distribution along overhead transmission lines' conductors and their resulting electric field*, Electrical Power and Energy Systems, vol. 108, pp. 198–210 (2014).
- [2] Dein A.Z., *Optimal Arrangement of Egyptian Overhead Transmission Lines' Conductors Using Genetic Algorithm*, Electrical Engineering, pp. 1049–1059 (2013).
- [3] Deželak K., Štumberger G., Jakl F., *Arrangements of overhead power line conductors related to the electromagnetic field limits*, Modern Electric Power Systems, pp. 13.2–13.7 (2010).
- [4] Szafrowski D., Bieńkowski P., Gumiela J., *Minimization of electric field intensity of 110 kV overhead power lines by purposeful configuration of phase wires*, Electrical Review (in Polish), pp. 170–174 (2017).
- [5] Salameh M.S.H., Al Nejdawi I.M., Alani O.A., *Using the nonlinear particle swarm optimization (PSO) algorithm to reduce the magnetic fields from overhead high voltage transmission lines*, International Journal of Research and Reviews in Applied Sciences, pp. 18–31 (2010).
- [6] Ranković A., Mijailović V., Rozgić D., Četenović D., *Optimization of Electric and Magnetic Field Emissions Produced by Independent Parallel Overhead Power Lines*, Serbian Journal of Electrical Engineering, vol. 14, pp. 199–216 (2017).

- [7] Ranković A., *Novel Multi-Objective Optimization Method of Electric and Magnetic Field Emissions from Double-Circuit Overhead Power Line*, European Transactions on Electrical Power, vol. 27, no. 2, p. 2243 (2017).
- [8] Książkiewicz M., *Passive loop coordinates optimization for mitigation of magnetic field value in the proximity of a power line*, Computer Applications in Electrical Engineering, pp. 77–87 (2015).
- [9] Deželak K., Štumberger G., Jakl F., *Optimization Based Reduction of the Electromagnetic Field Emissions caused by the Overhead Lines*, Electrical Review, vol. 87, no. 3, pp. 33–36 (2011).
- [10] Eberhart R.C, Shi Y., *Comparing inertia weights and constriction factors in particle swarm optimization*, Proceedings of the IEEE Congress Evolutionary Computation, pp. 84–88 (2000).
- [11] Whitacre J.M., *Recent trends indicate rapid growth of nature-inspired optimization in academia and industry*. Computing, vol. 93, pp. 121–133 (2011).
- [12] Whitacre J.M., *Survival of the flexible: explaining the recent dominance of nature-inspired optimization within a rapidly evolving world*, Computing, vol. 93, pp. 135–146 (2011).
- [13] Kalyanmoy D., Nikhil P., *Enhancing Performance of Particle Swarm Optimization through an Algorithmic Link with Genetic Algorithms*, Computational Optimization and Applications, vol. 57, pp. 761–794 (2014).
- [14] Budnik K., Machczyński W., *Contribution to studies on calculation of the magnetic field under power lines*, European Transactions on Electrical Power ETPE, vol. 16, pp. 345–364 (2006).
- [15] Djalel D., Mourad M., *Study of the influence high-voltage power lines on environment and human health (case study: The electromagnetic pollution in Tebessa city, Algeria)*, Journal of Electrical and Electronic Engineering, pp. 1–8 (2014).
- [16] Radwan R.M., Mahdy A.M., Abdel-Salam M., Samy M.M., *Investigate and Study the Effect of Electromagnetic Radiations Emitted from 400 kV High Voltage Transmission Lines on Human Health*, Tikrit Journal of Pure Science, pp. 135–139 (2013).
- [17] Baishya M.J., Kishore N.K., Bhuyan S., *Calculation of Electric and Magnetic Field Safety Limits Under UHV AC Transmission Lines*, Power Systems Conference (NPSC), Eighteenth National, IEEE, pp. 1–6 (2014).
- [18] Regulation of the Minister of the Environment of October 30, 2003 on the permissible levels of electromagnetic fields in the environment and ways to check compliance with these levels, Dz.U. no. 192 (in Polish), poz. 1883, 14 November (2003).
- [19] Salameh M.S.H., Al Hassouna M.A.S., *Arranging overhead power transmission line conductors using swarm intelligence technique to minimize electromagnetic fields*, International Journal of Research and Reviews in Applied Sciences, vol. 26, pp. 213–236 (2010).
- [20] Singer H, Steinbigler H., Weiss P., *A charge simulation method for the calculation of high voltage fields*, IEEE Trans. on PAS, vol. 93, iss. 5, pp. 1660–1667 (1974).
- [21] Modrić T., Vujević S., Lovrić D., *3D Computation of the Power Lines Magnetic Field*, Progress In Electromagnetics Research M, vol. 41, pp. 1–9 (2015).
- [22] Mamishev A.V., Nevels R.D., Russel B.D., *Effects of Conductor Sag on Spatial Distribution of Power Line Magnetic Field*, IEEE Trans. on Power Delivery, vol. 11, no. 3, pp. 1571–1576 (1996).
- [23] Vujevic S., Lovric D., Modrić T., *Segmentation of overhead power line conductors for 3D electric and magnetic field computation*, 10th International Conference on Applied Electromagnetics – PES 2011, Niš, Serbia (2011).
- [24] Deželak K., Štumberger G., Jakl F., *Emissions of electromagnetic fields caused by sagged overhead power lines*, Electrical Review, pp. 29–32 (2011).

- [25] Razavipour S.S., Jahangiri M., Sadeghipoor H., *Electrical Field around the overhead Transmission Lines*, World Academy of Science, Engineering and Technology, pp. 11–14 (2012).
- [26] Ztoupis I.N., Gonos I.F., Stathopoulos I.A., *Calculation of power frequency fields from high voltage overhead lines in residential areas*, 18th International Symposium on High Voltage Engineering, Seoul, Korea, pp. 61–66 (2013).
- [27] Khalid A.M., *Investigate and study the effect of electromagnetic radiations emitted from 400 kV high voltage transmission lines on human health*, Tikrit Journal of Pure Science, pp. 135–139 (2013).
- [28] Samy M.M., Radwan R.M., Mahdy A.M., Abdel-Salam M., *Electric field mitigation under extra high voltage power lines*, IEEE Transactions on Dielectrics and Electrical Insulation, pp. 54–62 (2013).
- [29] Baishya M.J., Kishore N.K., Bhuyan S., *Calculation of Electric and Magnetic Field Safety Limits under UHV AC Transmission Lines*, Power Systems Conference (NPSC), Eighteenth National, Guwahati, India (2014).
- [30] Fernandez J.C., Soibelzon H., *The surface electric field of catenary high voltage overhead transmission lines*, J. EMC and Power System, pp. 22–26 (2015).